LIQUID COOLING OF A MICROPROCESSOR: EXPERIMENTATION AND SIMULATION OF A SUB-MILLIMETER CHANNEL HEAT EXCHANGER

Fontaine J.[1], Gonzalez C.[1,2], Kumar P.[2], Pigache F.[1], Lavieille P.[1], Topin F.[2] and Miscevic M.[1]*
[1]University of Toulouse, LAPLACE (Laboratory on Plasma and Conversion of Energy), Toulouse, France
[2]Aix-Marseille University-CNRS, Laboratory IUSTI, Marseille, France
*Author for correspondence
University of Toulouse, LAPLACE (Laboratory on Plasma and Conversion of Energy),
UPS-INP-CNRS,
118 route de Narbonne,
31062 Toulouse Cedex 09, France
E-mail: marc.miscevic@laplace.univ-tlse.fr

NOMENCLATURE

c_p	[J/kg.K]	Specific heat capacity
D	[m]	Diameter
D_h	[m]	Hydraulic diameter
e	[m]	Thickness of the mini channel
g	[m/s^2]	Gravity acceleration
G	[W/K]	Thermal conductance
k	[W/mK]	Thermal conductivity
ℓ	[m]	Channel width
$\dot{m}$	[kg/s]	Mass flow rate
P	[Pa]	Pressure
Re	[-]	Reynolds number
t	[s]	Time
T	[K]	Temperature
u	[m/s]	Velocity

Special characters

ρ	[kg/m^3]	Density
μ	[Pa.s]	Dynamic viscosity
ξ	[-]	Singular pressure drops coefficient

Subscripts

c	Channel
f	Fluid (water)
t	Tube
w	Wall

ABSTRACT

A heat exchanger dedicated to the cooling of a microprocessor has been designed and realized. This heat exchanger consists of a bottom wall in contact with the processor and a cover that has been dug to a depth of 200μm on one side and 1 mm on the other side. Thus, by turning the cover, the hydraulic diameter of the channel can be changed. This heat exchanger has been experimentally tested both from hydraulic and thermal performances point of view. At the same time, 3D numerical simulations were carried out using commercial software based on finite volume method (StarCCM+) on a virtual model of the experimental prototype. Comparisons between numerical and experimental results are in good agreement. In particular, the influence of the distributor and the collector on the distribution of fluid flow and heat fluxes is emphasized.

INTRODUCTION

The evacuation of the heat generated within a microprocessor is a crucial problem. It affects the user from various points of view: limitation of performance and maximum temperature of the environment in which it can be used, drastic reduction in reliability and lifetime, energy consumption of the chip. It is therefore necessary to develop efficient cooling solutions in order to limit the temperature of a microprocessor even for high heat generation and to keep it near its optimum operating temperature.
Numerous works have been conducted to propose new techniques to enhance heat transfer and improve existing ones [1]. For application in high dissipative electronics, air cooling appears to be increasingly inappropriate as the low conductivity of the fluid in the gaseous state implies a low heat transfer coefficient. Thus, liquid or two-phase thermal management systems must be developed.

Furthermore, in addition to the rapid increase in the power density, electronic packages are more and more miniaturized, implying to develop efficient cooling systems with micro channels [2]. Yang et al. [3] have proposed a general optimization process for the thermo-hydraulic performances of mini-channel heat sinks. They reported empirical correlations extracted from literature and gave some recommendations about their use for practical design. Although many works have already been carried out, thermo-hydraulic behavior and performances of such miniature heat sinks are still to be explored [4; 5].

In this context, a heat exchanger prototype was designed and realized. The aim of this paper is to determine the ability of this liquid heat exchanger to cool a microprocessor. For that purpose, specific experiments and numerical simulations have been performed. The results obtained both experimentally and numerically with this low hydraulic diameter heat exchanger are presented and compared in the next sections.

EXPERIMENTAL SETUP

Heat exchanger

The exchanger consists of two parts, the sole and the cover, made of copper and aluminum, respectively. Two grooves are machined in the sole and communicate with the inlet and outlet pipes (see fig. 1). An O-ring is placed at the periphery for sealing.

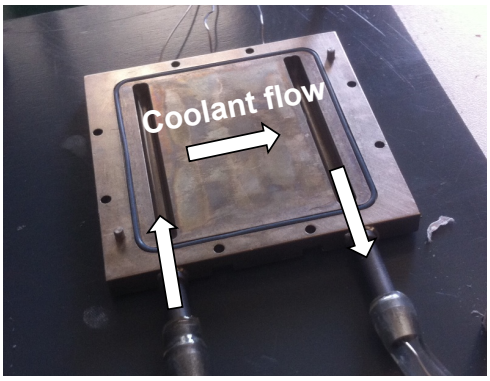

Figure 1. Photograph of the bottom wall of the heat exchanger, made of copper. The two grooves constitute the manifolds.

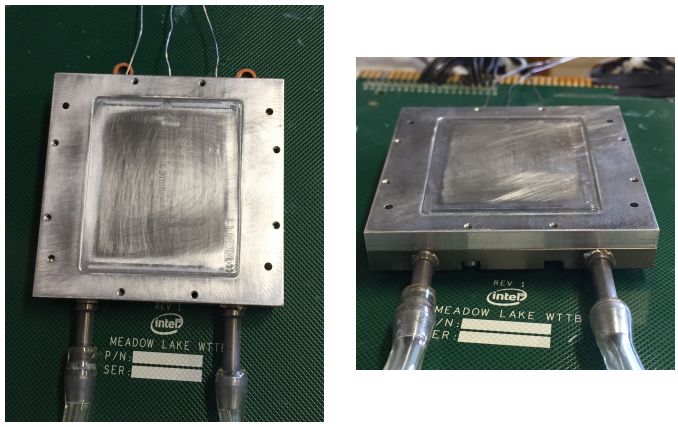

Figure 2. Photographs of the heat exchanger after assembly: - left : top view (dug cover) - right : side view

The cover is a simple parallelepiped plate which has been dug to a depth of 200 μm on one face and 1 mm on the other face. Thus, by turning the cover, the hydraulic diameter of the channel can be changed. The channel obtained for the circulation of the fluid after assembly is thus rectangular in cross-section of 50 mm in width, 38 mm in length (distance between the distributor and the collector) and is 200 μm or 1 mm in height (Fig. 2).

In order to be able to determine the thermal performance independently of the thermal contact resistance between the exchanger and the microprocessor, three thermocouples are inserted into the sole at a distance of 1 mm from the surface in contact with the fluid. The thermocouples are K-type, sheathed in stainless steel, 0.5 mm in diameter. The holes in the sole were made by electroerosion; they have a diameter of 0.6 mm and a length of 33 mm. Two other thermocouples, identical to the previous ones, are placed in inlet and outlet pipes of the heat exchanger in order to measure the inlet and outlet temperatures of the fluid. Accuracy on temperature measurements is estimated to be 0.1°C (after calibration). A differential pressure sensor is positioned between the inlet and outlet pipes of the heat exchanger (the connections of the pressure sensor to the loop are located 25 cm upstream and downstream of the inlet and outlet pipes of the heat exchanger, see fig. 4) and allows measuring the pressure loss with an accuracy of less than 10 Pa.
The heat exchanger thus built was tested experimentally by placing it on a microprocessor mock-up supplied by Intel company. This mock-up is geometrically identical to a commercially available processor and generates similar and easily modulable thermal sollicitations.

Test bench

The heat exchanger is connected to a hydraulic circuit (see schema in fig. 3 and photos in fig. 4 and 5). A counter-current tubular heat exchanger is used as cold source for the fluid loop.

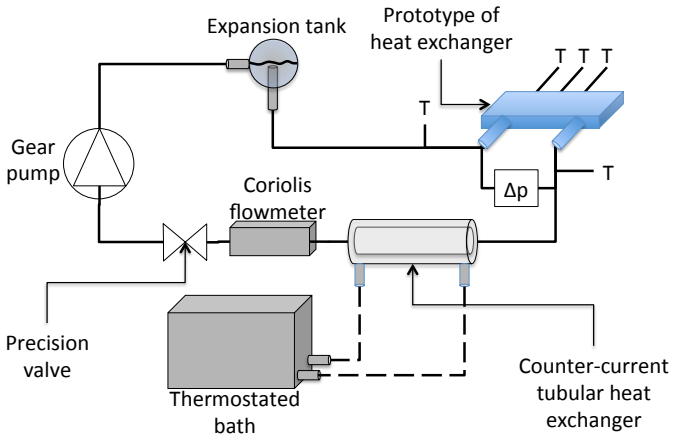

Figure 3. Sketch of the experimental apparatus.

The fluid then passes through a Coriolis flowmeter allowing mass flow rate measurements in the range 0-3 $g.s^{-1}$ with an accuracy of 0.01 $g.s^{-1}$. A mechanical pump (gear pump) whose rotational speed can be modulated is then used for discharging the fluid into a precision valve. This latter allows modulate the pressure drop in the circuit at the desired value in a simple manner. The fluid then flows toward the inlet of the heat exchanger prototype. A reservoir (open to the atmosphere) is connected to the hydraulic circuit and serves as an expansion vessel. The secondary fluid in this heat exchanger is cold thermostated water.

NUMERICAL SIMULATION

Simultaneously, direct numerical simulations of these exchangers were carried out using commercial software StarCCM+.The virtual prototype was constructed using the CAD modeling of the heat exchanger (bottom wall, top cover and

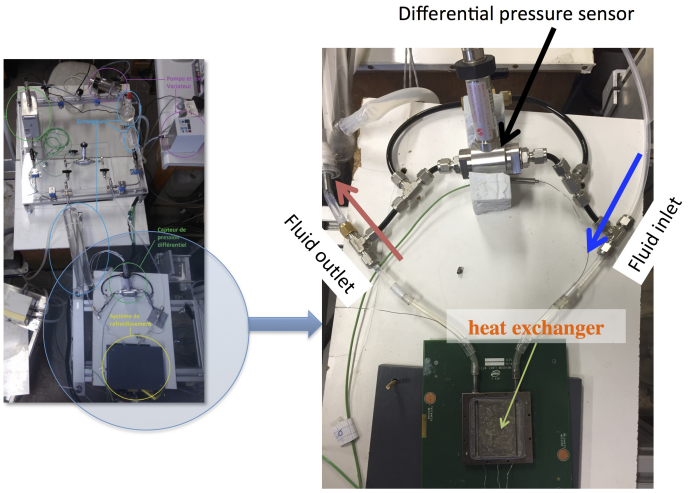

Figure 4. Top views of the experimental device: - left: the whole hydraulic circuit - right: zoom on the prototype placed the microprocessor mock-up and its connections to the loop.

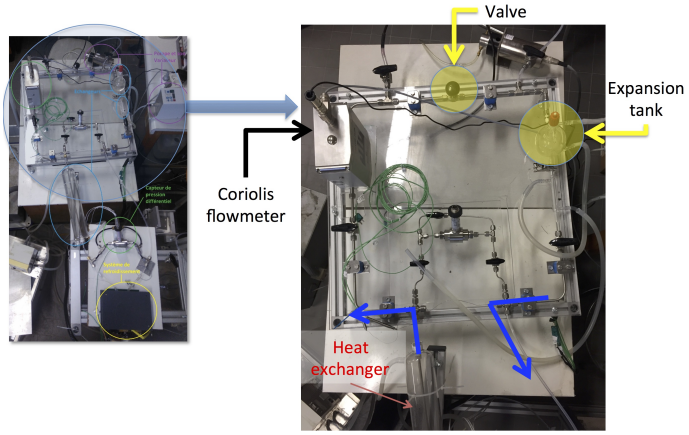

Figure 5. Top views of the experimental device: - left: the whole hydraulic circuit - right: zoom on the hydraulic circuit (Coriolis flowmeter, precision valve, gear pump, expansion tank).

channel). The conjugate heat transfer problem was solved in the transient regime, and heat conduction is considered in all solid parts. Note that a perfect thermal contact between top and bottom parts of the assembly was considered. For the channel, as well as inlet and outlet manifolds, the incompressible laminar and transient conjugate flow and heat transfer problems were solved using the classical combination of continuity, momentum and energy equations:

$$\vec{\nabla}\cdot\vec{u}=0 \tag{1}$$

$$\rho\frac{\partial\vec{u}}{\partial t}+\rho\left(\vec{u}\cdot\vec{\nabla}\right)\vec{u}=\rho\vec{g}-\vec{\nabla}\cdot\overline{\overline{P}}+\mu\Delta\vec{u} \tag{2}$$

$$\rho c_p\left(\frac{\partial T}{\partial t}+\vec{u}\cdot\vec{\nabla}T\right)+\rho\vec{u}\cdot\frac{\partial\vec{u}}{\partial t}+\frac{\rho}{2}\left(\vec{\nabla}\|\vec{u}\|^2\right)\cdot\vec{u}=k\Delta T+\frac{\partial P}{\partial t} \tag{3}$$

The physical properties of the fluid were considered to vary with the temperature (water using the models of IAPWS-IF97 (International Association for the Properties of Water and Steam, Industrial Formulation 1997)) while the solid part properties are supposed constant (copper for the base and aluminium for the top cover). The numerical resolution used a segregated approach with implicit second order temporal discretization and ad hoc relaxations factors in order to obtain adequate convergence behavior. 1691272 and 1852205 meshes were used for the 1 mm and the 200 μm heat exchanger, respectively. For both cases, an unstructured trimmer - octree mesh structure is used, save for the channel where structured hexahedral anisotropic cells are used with 16 up to 20 cells along the height of the channel. This mesh is refined in the vicinity of all solid-fluid interface and near inlet and outlet of the channel. Mesh convergence effects were checked and no additional improvement is obtained with further refinement.

Both mass flow rate and fluid temperature were imposed at the inlet of the heat exchanger, while at the outlet the pressure is imposed to the atmospheric one. A uniform heat flux is imposed on the bottom wall of the sole, on a area of 30×30 mm^2 as in the experiments. The rest of the solid walls are considered adiabatic (as experimental results show that thermal losses are negligible).

RESULTS

Hydraulic behavior

A first series of experimental tests and numerical simulations were carried out without powering the processor, at a temperature of 20°C, in order to characterize the heat exchanger from hydraulic point of view. The pressure losses obtained as a function of the mass flow rate are reported in Fig. 6 for the two channel thicknesses considered (200 μm and 1 mm).

Globally, experiments and numerical simulations exhibit the same trend. Nevertheless, significant discrepancies are found between experimental and numerical results, especially for the 1 mm channel. These discrepancies can be explained by the fact that the pressure losses in the numerical simulations are determined between the inlet and the outlet of the heat exchanger, while in the experiments the tappings for the pressure measurement are located at 25 cm upstream and 25 cm downstream of the prototype. Thus, additional pressure losses are taken into account in the experiments (regular pressure drop in the inlet and outlet tubes, as well as singular pressure drops in the connections between the tubes of the loop and the heat exchanger). Furthermore, in the 1 mm channel heat exchanger, the flow distribution appears less homogeneous than in the 200 μm channel heat exchanger, as it can be seen in fig. 7 and fig. 8, respectively. For the 1 mm channel heat exchanger, the flow distribution could be homogenized by optimizing the distributor and collector headers as suggested, for instance, by Saeed and Kim [6]. From these fig-

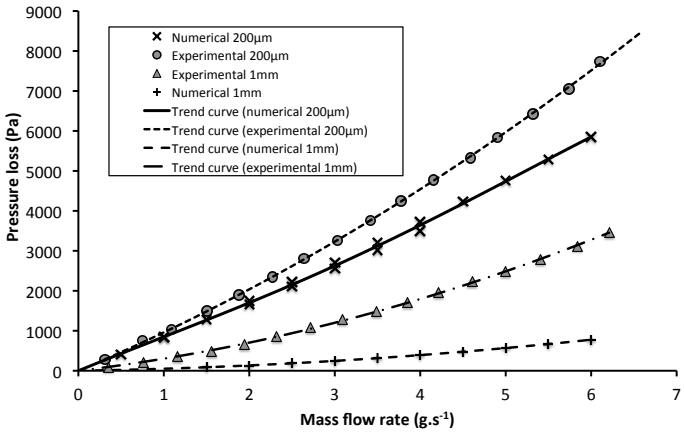

Figure 6. Experimental and numerical pressure losses as a function of the mass flow rate for the two channel thicknesses.

ures, it can be speculated that the main part of the pressure drop in the 200 μm channel heat exchanger is the regular pressure drop in the channel itself, while in the 1 mm the main part of the pressure drop corresponds to the pressure drop in the singularities and in the manifolds.

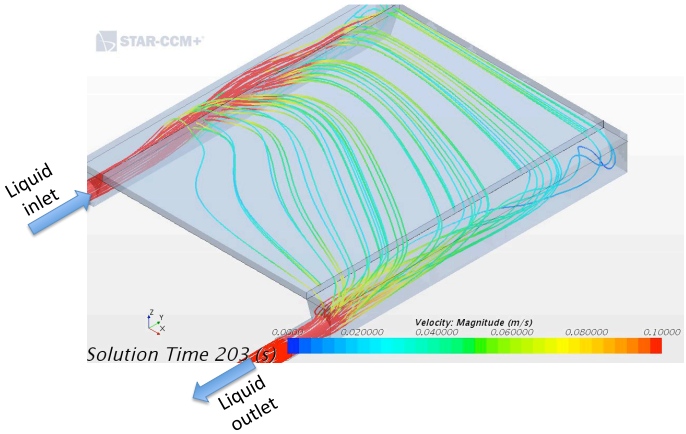

Figure 7. Calculated streamlines in the 1 mm channel heat exchanger in adiabatic configuration. The liquid temperature is 20°C.

To assess the respective contributions of the channel and the singularities on the total pressure drop, an analytical estimation can be done. Assuming a Poiseuille flow in the inlet and outlet tubes, as well as in the channel, the pressure drop can be calculated as:

$$\Delta p = \frac{64}{Re_{D_t}}\frac{L_t}{D_t}\frac{1}{2}\rho U_t^2 + \frac{64}{Re_{Dh}}\frac{L_c}{D_h}\frac{1}{2}\rho U_c^2 + \sum_i \xi_i \frac{1}{2}\rho U_c^2 \quad (4)$$

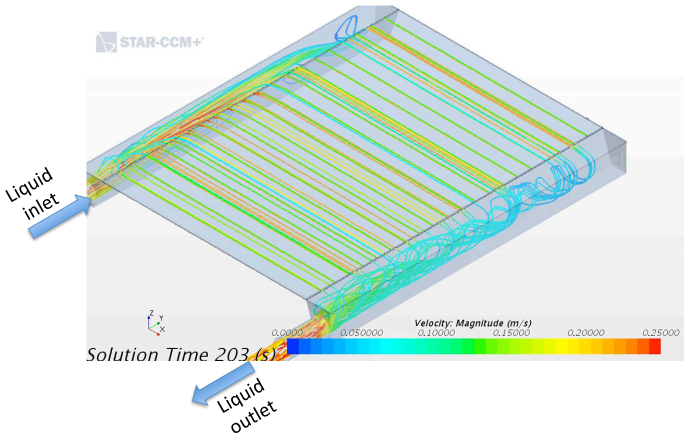

Figure 8. Calculated streamlines in the 200 μm channel heat exchanger in adiabatic configuration. The liquid temperature is 20°C.

With:

$$Re_{D_t} = \frac{\rho U_t D_t}{\mu} \quad (5)$$

and

$$Re_{D_h} = \frac{\rho U_c D_h}{\mu} \quad with \quad D_h = \frac{4e\ell}{2(e+\ell)} \approx 2e \quad (6)$$

The last term in equation 4 represents the pressure drop due to all the singularities. The value of $\sum_i \xi_i$ is adjusted to reproduce the experimental pressure drop of the 1 mm channel heat exchanger:

$$\sum_i \xi_i \approx 5 \quad (7)$$

The pressure losses in the 200 μm channel heat exchanger are 2 to 2.5 times higher than those measured with the 1 mm channel heat exchanger, while the hydraulic diameter is 5 times lower. This behavior can be explained by analyzing the part of the regular pressure losses in comparison with the singular pressure losses corresponding to the different changes in flow direction and cross-sections. These relative contributions are shown in fig. 10 and 11. For the 1 mm channel heat exchanger, the pressure losses in the actual channel are negligible, less than 2% of the total pressure losses. For the exchanger with the 200μm channel, these pressure losses in the channel become preponderant and represent 60 to 70% of the total pressure losses.

Thermal performance

In order to determine the heat performance of the two configurations of the heat exchanger, specific tests were carried out.

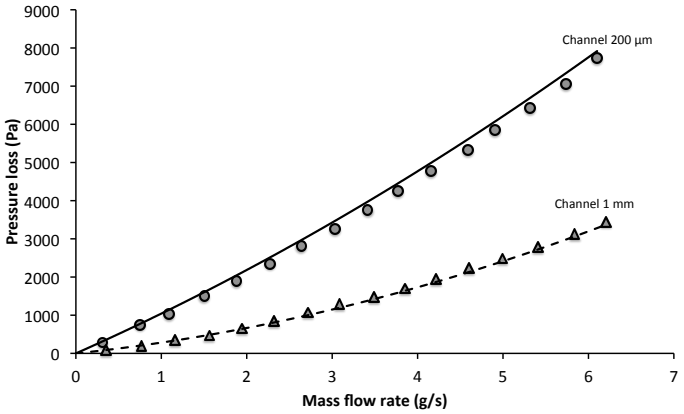

Figure 9. Variation of the pressure loss in the heat exchangers as a function of the mass flow rate. The symbols are the results obtained experimentally; The lines are the results given by Eq. 4 with $\sum_i \xi_i = 5$.

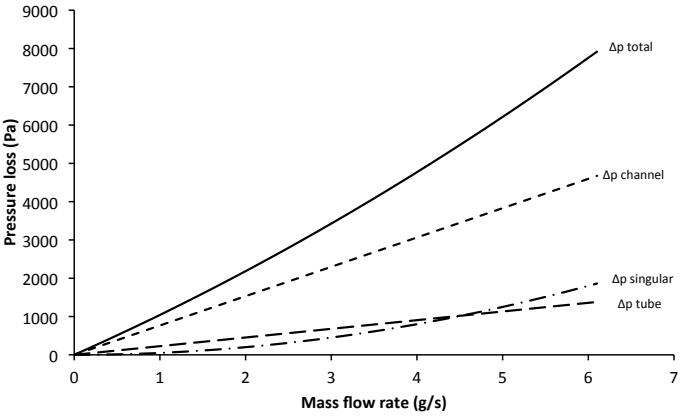

Figure 10. Comparison between regular and singular pressure drops in the 200 μm channel heat exchanger. Δp_{tube} represents the pressure drop in the 25 cm upstream tube and the 25 cm downstream tube.

The experimental protocol consists in imposing a water flow rate by means of the gear pump and then supplying the microprocessor simulator with an electrical power such that the water temperature difference between the inlet and the outlet is equal to 10 ± 0.2°C. The inlet temperature of the water in the exchanger is imposed at 23.5°C for all the tests carried out. The deviations between the applied electric power and the heat flux received by the water (quantified by multiplying the mass flow rate with the enthalpy variation) vary between 0 and 7%, and are on average 4%.

The mean temperature $< T_w >$ of the bottom wall of the heat exchanger is evaluated by performing a 2^{nd} order polynomial regression of the measured wall temperatures and then integrating this regression between the inlet and the outlet of the channel (i.e. between the outlet of the distributor and the inlet of the collector,

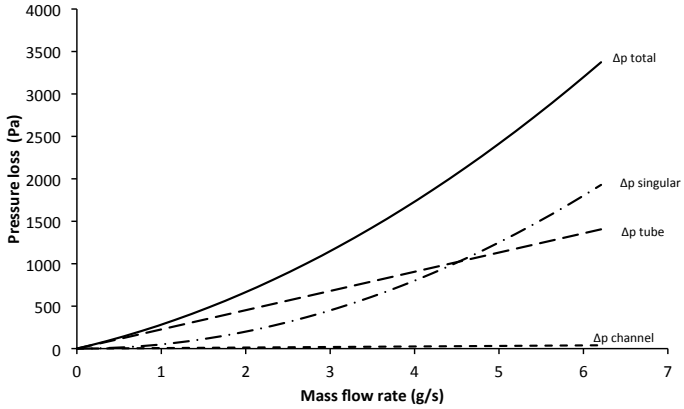

Figure 11. Comparison between regular and singular pressure drops in the 1 mm channel heat exchanger. Δp_{tube} represents the pressure drop in the 25 cm upstream tube and the 25 cm downstream tube.

on a distance of 38 mm). It should be noted that this calculation represents only an estimation of the mean temperature because it does not take into account the 2-D distribution of the surface temperature (variation in the direction perpendicular to the main axis of the flow). The average fluid temperature $< T_f >$ is estimated by performing an arithmetic mean between the inlet and outlet water temperatures. Considering the operating conditions described above, this average temperature of the water in the heat exchanger is substantially constant for all the experiments and is equal to 28.5°C. An "apparent" overall thermal conductance G of the heat exchanger is then defined as:

$$G = \frac{\dot{m} c_p (T_{out} - T_{in})}{< T_w > - < T_f >} \tag{8}$$

The variations of this apparent overall thermal conductance as a function of the mass flow rate are shown in fig. 12 for the two channel thickness values considered.

As it can be seen from this figure, the thermal conductance of the 200 μm channel heat exchanger is substantially higher than that of the 1 mm channel heat exchanger: enhancement up to 70% is achieved for mass flow rate approximately equal to 3 g/s. For such a mass flow rate, the overall thermal conductance of the 200 μm channel heat exchanger is almost 15 W/K. So, considering water as the working fluid, and a 10°C fluid temperature difference between inlet and outlet, heat flux up to 125 W can be removed from the microprocessor. In that case, the temperature of the bottom wall of the heat exchanger would be only about 8°C higher than the fluid mean temperature. It can thus be concluded that such a heat sink can be efficiently integrated to applications such as microprocessor thermal management.

Numerical simulations have been performed in the same conditions than the experiments (i.e. inlet water temperature equal to 23.5°C, applied heat flux adjusted to obtain a water temperature difference between inlet and outlet equal to 10°C). In order

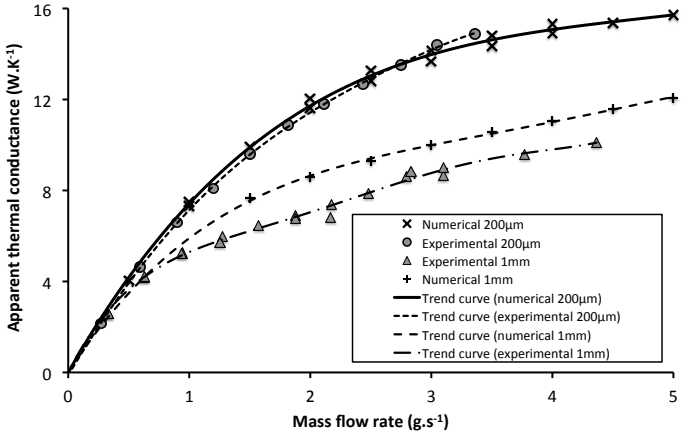

Figure 12. Variation of the apparent thermal conductance as a function of the mass flow rate for the two channel thicknesses. The same procedure is applied to calculate G (eq. 8) from the experiments and the numerical simulations.

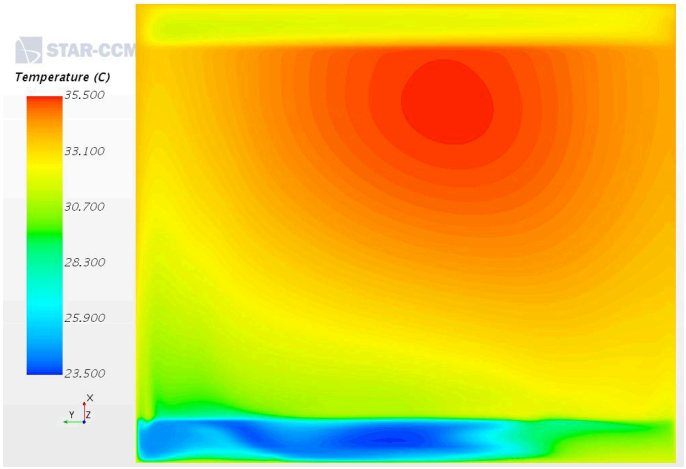

Figure 14. Temperature field of the water at mid-height of the 1 mm channel. The inlet temperature is 23.5°C, the mass flow rate is 1.5 g/s and the heat flux is 62.7 W.

to be able to compare the experimental and numerical results, virtual temperature sensor are placed at the same locations than the experimental ones and data are extracted from the numerical temperature field. The same procedure than the one used in the experiments is then applied to calculate the apparent overall thermal conductance. The results obtained with this procedure are reported on the same figure than the ones obtained from experiments (fig. 12).

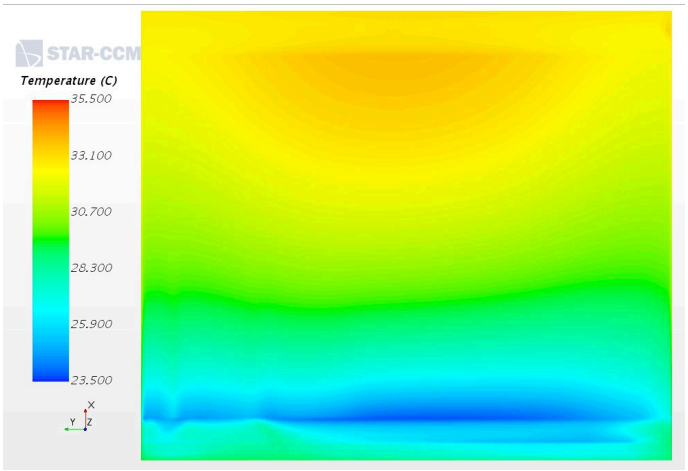

Figure 13. Temperature field of the water at mid-height of the 200 μm channel. The inlet temperature is 23.5°C, the mass flow rate is 1.5 g/s and the heat flux is 62.7 W.

Adequacy between experimental and numerical results is excellent for the 200 μm channel heat exchanger, while the numerical simulations slightly overestimate the overall thermal conductance in the case of the 1 *mm* channel heat exchanger. As mentioned in the hydraulic behavior section, the flow in the 1 mm channel is non-uniformly distributed. This maldistribution of the flow implies that the temperature field of the fluid in the case of the 1 mm channel is farther from a one-dimensional field than in the case of the 200 μm channel (see fig. 13 and fig. 14). Calculating the mean temperature of the fluid by integrating a second order polynomial trend curve as described above is therefore less precise in the case of the 1 mm channel than in the case of the 200 μm channel. In the case of the 1 mm channel heat exchanger, the flow field is more sensitive to the deviation in the imposed inlet conditions and geometry compared to the real ones. It is thus not surprising to obtain a better match between numerical results and experiments in the case of the best distributed flow.

CONCLUSION

An experimental setup and a numerical tool have been built in order to analyse hydrothermal performances of heat sink with low diameter channel. For the 1 mm channel heat exchanger, it was found that the main contribution in the pressure drop is due to the singularities and the tubes upstream and downstream of the heat exchanger, and that the flow is badly distributed in the channel. For the 200 μm channel, the main contribution in the pressure drop is due to the pressure loss in the channel itself, and the maldistribution is not significant. From heat transfer point of view, the 200 μm channel heat exchanger allows reaching thermal conductance up to 15 W/K with a very low mass flow rate of 3 g/s. This thermal performance demonstrates that such a liquid cooling heat sink could be efficiently used for the thermal management of electronic chip like microprocessor.

ACKNOWLEDGMENT

This work has been realized in the framework of the CANOPEE project and supported by the "Fond Unique Interministériel (FUI) - 18th call for projects". We gratefully acknowledge contributions from all project partners.

REFERENCES

[1] Léal L., Miscevic M., Lavieille P., Amokrane M., Pigache F., Topin F., Nogarède B., Tadrist L., An overview of heat transfer enhancement methods and new perspectives : focus on active methods using electroactive materials, *Int. J. Heat Mass Transf.*, vol. 61, 2013, pp. 505-524.

[2] Xie X.L., and Liu Z.J., and He Y.L., and Tao W.Q., Numerical study of laminar heat transfer and pressure characteristics in a water-cooled minichannel heat sink, *Applied Thermal Engineering*, vol. 29, 2009, pp. 64-74.

[3] Yang X.H., and Tan S.C., and Ding Y.J., and Liu J., Flow and thermal modeling and optimization of micro/mini-channel heat sink, *Applied Thermal Engineering*, vol. 117, 2017, pp. 289-296.

[4] Dixit T., Ghosh I., Review of micro- and mini-channel heat sinks and heat exchangers for single phase fluids, *Renewable and Sustainable Energy Reviews*, vol. 41, 2015, pp. 1298-1311.

[5] Ghani I.A., Sidik NAC, and Kamaruzaman N, Hydrothermal performance of microchannel heat sink: The effect of channel design, *International Journal of Heat and Mass Transfer*, vol. 107, 2017, pp. 21-44.

[6] Saeed M., and Kim M.H., Header design approaches for mini-channel heatsinks using analytical and numerical methods, *Applied Thermal Engineering*, vol. 110, 2017, pp. 1500-1510.